The 2009 IEEE/RSJ International Conference on
Intelligent Robots and Systems
October 11-15, 2009 St. Louis, USA

Micro-to-Nano Optical Resolution in a Multirobot Nanobiocharacterization Station

J. Otero, M. Puig-Vidal, *Member, IEEE,* M. Frigola, *Member, IEEE* and A. Casals, *Senior Member, IEEE*

***Abstract*—A multi-robot cooperation station for nano-bio characterization of biological specimens is presented. The station is composed of two long travel range and high resolution robots equipped with self-sensing nanoprobes that are able to cooperate with each other and with standard AFM systems, over a common sample. The robots are guided by the use of an upright high-depth-of-field optical microscope to perform complex nano-bio characterization experiments. To achieve the required precision between the two robots reference frames, specific image processing techniques are needed. One of the tips is dedicated to acquire the topography of the sample at nano scale while the second probe performs the biocharacterization experiments. The obtained results show that the two robots can cooperate within the required resolution in bacterial nanomechanical characterization while high resolution topographic images are acquired.**

I. Introduction

ATOMIC Force Microscopy (AFM) technique is of high interest in biology and medicine because it can be used for nanometric resolution imaging, to study nanomechanical and biochemical properties and to nanomanipulate the surface of biological samples under physiological conditions [1]. The techniques used for such applications are based on measuring the interaction forces between a very sharp tip (nanometric radius) and the sample surface with nN-pN resolution [2]. This extremely high resolution in the measurement and control of interaction forces allows the study of nanomorphologic and nanomechanical properties of living cells (and, in general, of very soft matter) without damaging them. In addition, the information extracted from such detailed measurements allows researchers to investigate subcellular parts and even biomolecules such as proteins or DNA [3], [4].

Unfortunately, AFM characterization techniques still have several limitations, where possibly the main drawback is the use of the same probe to study different characteristics (for instance, morphology, elasticity and the surface proteins distribution) of a sample in the same experiment. Therefore, a good trade-off can be achieved using a probe that although is not optimum for each experiment, it is still good enough for all of them for the concrete application requirements. However, the use of a unique probe prevents the use of very high sensitivity force cantilevers (their very low spring constant difficult the imaging procedure) and functionalized tips (with an active biolayer for the measurement of biochemical interactions in the surface) if high resolution imaging is a requirement in the experiment. Another main limitation of bio-oriented AFM microscopes is that manufacturers usually mount an inverted optical microscope to avoid the need of dealing with working distance related engineering problems: the mechanical design of the head should allow the approaching of the objective to the sample with the probe over it, so the working distance need to be longer than the one required in the inverted solution. In most experiments, the operator needs the use of the information given by the optical microscope to go from the microworld to the nanoworld (micro-to-nano integration); for that reason substrates are limited to transparent ones, that is: materials of interest in biomedicine such as gold or titanium [5] are not suitable for this working mode; for high resolution imaging (protein imaging, DNA, etc.), the substrates should be atomically flat (HOPG, mica, etc.) and the inverted optical microscope can neither be used in this case.

On the other hand, advances in microrobotics technology have demonstrated that robots are able to perform experiences based on AFM techniques when equipped with self-sensing probes [6]. The goal is having micro- and nano-robots equipped with self-sensing nanotools that are capable of cooperating with each other and with other systems using standard tools to operate in complex experiments. Thus, robots open the door to avoiding current problems when using standard one-probe solutions.

To overcome the above mentioned problems, a robotic station has been implemented. It is composed of two long travel range and high resolution robots equipped with self-sensing nanoprobes [7]. The robots are guided from an upright high-depth-of-field optical microscope to perform complex nanobiocharacterization experiments. One of the tips is dedicated to acquire the topography of the sample while the second probe performs the nanocharacterization experiments. This second probe (which is free from the topography task) can be, then, functionalized with a specific biochemical group; it also allows the use of a cantilever with

Manuscript received 1 March, 2009. This work was supported in part by the Spanish Ministerio de Ciencia e Innovación under Grant FPU AP2006-01079.

J. Otero and M. Puig-Vidal are with the Barcelona University UB. Corresponding author e-mail J. Otero:jotero@el.ub.es.

M. Frigola and A. Casals are with the Bio-Engineering Institute of Catalonia (IBEC) and Technical University of Catalonia (UPC)

very low spring constant or a non-AFM tool (a nanoelectrode, microgripper, lithography probe...). A representation is shown in figure 1.

Although the range of complex experiments to be performed with the final station is wide, this first work is centered in nanocharacterization of bacterial cells when they form biofilms [8]. From the expected results, microbiologists will be able to correlate morphological studies [9] (high resolution imaging) and nanotribology tests [10] (with a functionalized probe) for a better understanding of the behavior of biofilms formation. Since the size of a bacteria is about 1µmx2µm (Figure 2), and taking into account that the first probe performs a high resolution scaning image, the second probe has to be positioned with respect to the first one with an optical resolution better than the lower radius of the bacteria, that is, 500 nm. In this way, it is possible to assure that the second probe is over the desired cell when performing the nanobiocharacterization experiment.

II. Materials and Methods

The nanobiocharacterization station based on two robots with their corresponding tips working cooperatively have to be calibrated and the two robot tips referred to a common reference frame. The following subsections describe the components of the experimental platform, the required image processing for tips localization and the absolute and relative reference frames.

A. The multiprobe robotized station

The multiprobe station developed consists of two robots working cooperatively under an upright optical microscope. The desired robot movements are achieved using microstepper motors and piezoelectric actuators. The two robots can be endowed with different nano-tools working cooperatively in the same window of the optical microscope. A picture of the whole robotic platform is shown in figure 3.

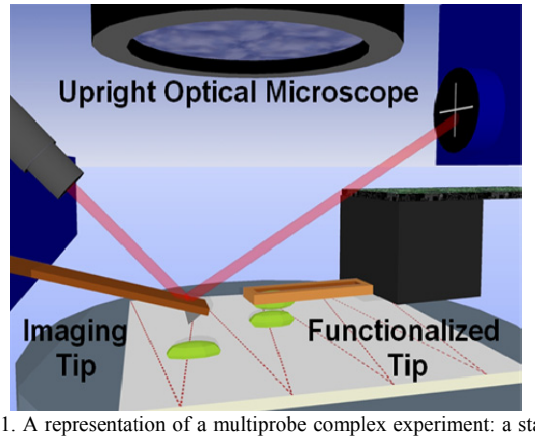

Fig 1. A representation of a multiprobe complex experiment: a standard AFM probe and a self-sensing functionalized tip

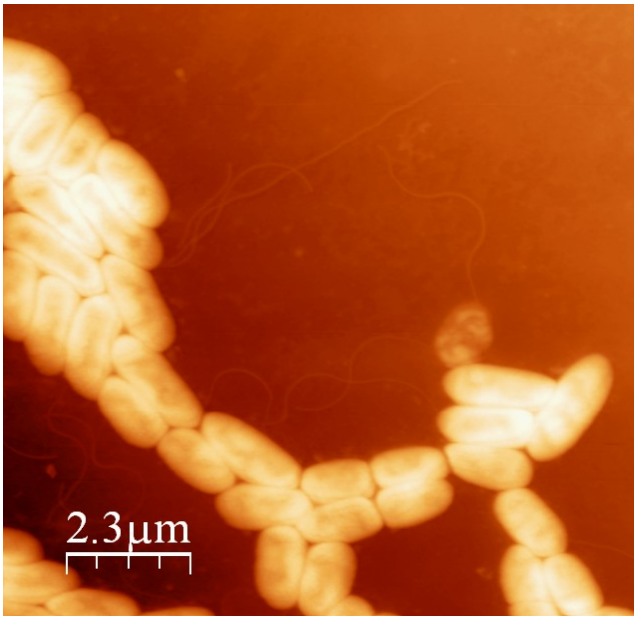

Fig 2. Pseudomonas Aureginosa in the early stages of biofilm formation over gold substrate imaged with an AFM standard probe (Olympus OMCL) with laser-photodiode measurement.

At the macro-micro range, the positioning is based on manual translation stages using stepper motors advancing at microsteps; this positioning technique works in open loop, so for closing the loop, there is an optical microscope with a CCD sensor. In the nanorange, the positioning is based on piezoelectric actuators in closed loop using strain gauge displacement sensors.

In the current platform, the robots are endowed with distance nanosensors based on quartz tuning forks and force nanosensors based on piezoresistive cantilevers [11]. The control system of the station is implemented using a meet-in-the-middle approach (in contrast to top-down or bottom-up approaches) to become robust but at the same time versatile enough to extend its use in future applications of the station.

The nanobiocharacterization station has three different positioning levels going from long range-low resolution to short range-high resolution, as shown in figure 4. This specific design is performed to accomplish long travel and high resolution uncoupling [12].

The resolution of each positioning level should be some orders of magnitude greater than the immediate following subsystem. The first positioning stage consists of manual positioning stages of 50 mm of travel and 1µm of resolution (accomplished in X and Y) with the use of the optical microscope and specific techniques of pattern recognition presented in this work. The second stage is based on microstepper motors, with a travel of 12 mm and a resolution of 100 nm. The fine positioning is done using closed loop piezoelectric actuators with a resolution of 2 nm and a bi-directional repeatability of 25 nm (Figure 4).

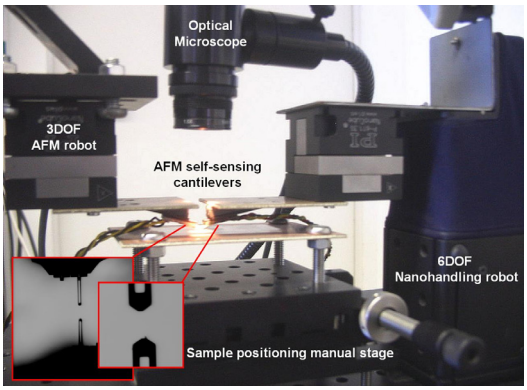

Fig. 3. The implemented nanobiocharacterization station.

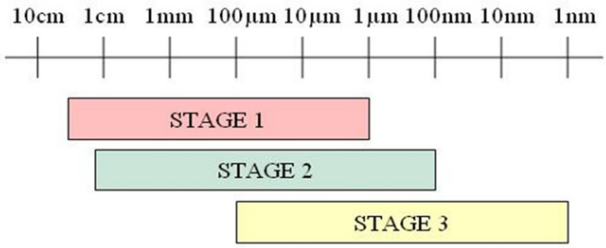

Fig. 4. Three levels of the station positioning subsystem, from travel range to resolution of each one. The uncoupling of the long range and high resolution is accomplished by the overlap area between stages (macro to micro to nano integration).

B. AFM tip localization in the optical microscope images

Developments in computer vision algorithms have made digital image techniques a popular tool for precise object localization. Several sub-pixel registration algorithms have been developed belonging to image registration category (see [15] for a complete survey). In order to localize several AFM tips in the same images, a sub-pixel segment-based registration technique is proposed.

At the micro-nano scale, and due to the image acquisition conditions: diffraction, non-mono chromatic illumination, wide field of view, relatively small lens' aperture and long focal distance with respect to the distance to the specimen; the borders of the objects appear strongly blurred. Under these image conditions sub-pixel accuracy is difficult to achieve. Fig. 5 shows an example of the impact of the blurring effect in a grey level image of one tip's edge (fig. 5a) and the typical 'S' shape of the grey level profile (fig. 5b) measured with respect to the edge's perpendicular direction.

An edge of the tip appears in figure 5a with a blurring effect of 12 pixels width. Taking into account that each pixel match approximately an area of 240 x 240 nm, the quality of the acquired images are far from the desired ones (theoretical Abbe limit). The noise level of the images, due to the low light intensity that reaches the CCD during the exposition time, is estimated to be about 10%. Moreover, the camera cannot be considered static or fixed; the whole camera vibrates producing an apparent displacement of the scenario between two successive images. In order to have an estimation of the vibrations amplitude to compensate their effects, an image is calculated from the integration of the difference between successive images.

Figure 6 shows the results of integrating the differences between 25 successive images while the background (square pattern) is maintained steady. Measured directly in the image difference, the camera tremor influence is in this case of about 3 pixels (0.75 µm approx).

When the movement is limited to just a translation between two images, the technique usually applied to measure displacements is cross correlation between images, by means of a fast Fourier transform [13]. In our case, due to the fact that the AFM tips can move in an independent way over a complex background, due to real time requirements and to the need of having a fixed point for frame correspondence, these techniques are difficult to use here. The implemented approach to localize objects in the images consists in a geometrical model matching technique based on image-gradient segment adjustment.

Before beginning the entire process of model adjustment and in order to reduce the noise of the original images, two filters are applied: a median filter and a Gaussian smoothing filter. After that, a gradient image $G(x,y)$ is computed for tool localization using model matching techniques.

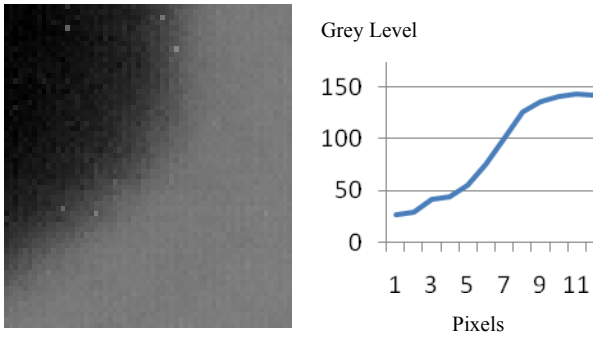

a) *b)*

Fig 5. Image conditions. a) Blurring effects in one corner of the AFM tip b) Grey level profile with respect to the edges' perpendicular direction.

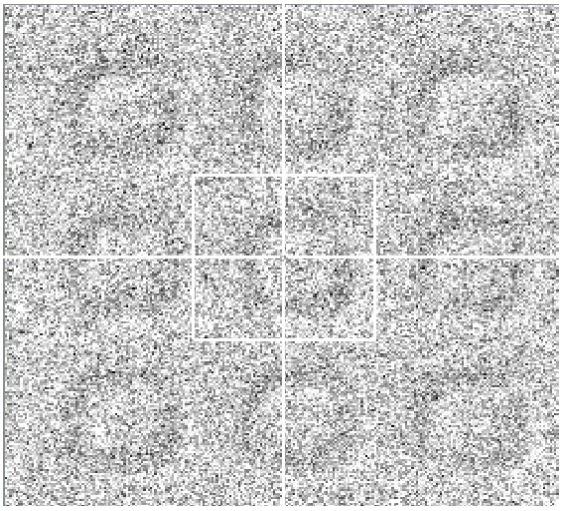
Fig. 6 Image difference integration results between successive images

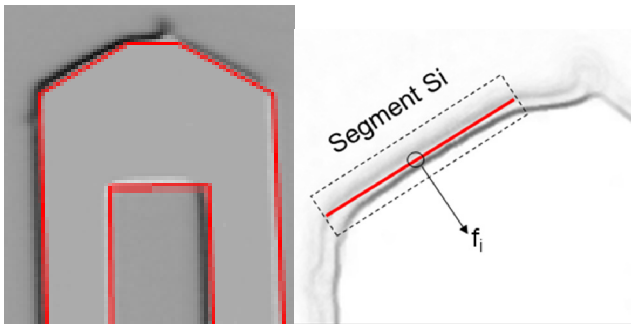

a) b)

Fig 7. Model of segments an AFM tip. a) Vectors based model, b) Virtual force (fi) applied to a segment using gradient images.

A geometrical model is used to describe the shape of the AFM tips (fig 7a). These geometrical models are constituted by a set of segments $M = \{S_1,...S_n\}$. Each segment S_i is defined by the image coordinates of the central point (p_i), its perpendicular normal vector (v_i) and its length (l_i). The method used to adjust the model consists in assigning a virtual dragging force (f_i) that pulls each segment S_i to a convergence position (fig. 7b). Each segment contributes with a dragging force f_i to move the model's position. Due to the fact that short segments have less significance than long segments, each force f_i is weighted proportionally to its corresponding segment l_i length. Iteratively, the model moves in an incremental way, getting its new position proportionally to the resultant of the whole forces (F). The process begins again with the new position of the model, until a given convergence level is obtained.

The expression of the resultant force vector F used to adapt the model to its new position has the following expression:

$$\vec{F} = \frac{1}{L}\sum_{i=0}^{n} l_i f_i \vec{v}_i \qquad L = \sum_{i=0}^{n} l_i \qquad (1)$$

Where L is the perimeter of the model. This expression (1) assures that an individual segment produces dragging forces only in its perpendicular direction (the direction in which a segment-matching algorithm is more able to sense). With the total resultant forces, a displacement vector (D) is calculated as $\vec{D} = k \cdot \vec{F}$. As usual in this kind of iterative procedures, the constant k must be kept small enough in order to avoid large oscillations, but also big enough to avoid too slow convergences.

A segment is considered well placed when it is in the middle of its corresponding slope in the gray images. Then, the method used to estimate the individual force components f_i of each segment relies on measuring the imbalance of the gradient image between the two sides of the segment. This imbalance is measured integrating (Eq.2) both sides of the segment in the gradient images, as:

$$f_i = \frac{1}{area_i}\sum_{\forall (x,y)\in[]} G(x,y)\cdot Sign(x,y,S_i) \qquad (2)$$

Where $G(x,y)$ represents the normalized module of the gradient of the input image, the function $Sign(x,y,S_i)$ returns +1 if the coordinates (x,y) are in the half positive space defined by the segment Si, and -1 otherwise. The value $area_i$ is the value of the area around the segment S_i (doted rectangle in fig 7b) indicated with the symbol [] in eq. 2.

C. *Optical scale factor and offset calibration*

Robot coordination relies on having a precise common reference frame. The two robots reference frames are related one to each other using the optical microscope. It is necessary to calibrate the arm-tool offset (fig. 8a), which is the distance between an arbitrary point of the AFM tip shape in images {Arm} and the effective place where the tool is under the cantilever {Tool}.

There are three different techniques:

1) Making a lithograph visible from the optical microscope to calibrate the position of the tip.
2) Making a scanning topographic image with the tool and then correlate it with the image obtained from the second tool.
3) Performing a pre-image of tips with the Scanning Electron Microscope.

The most effective technique seems to be the second one, because the first solution is dangerous for the tip and the third results in an incomplete calibration due to several uncertainties in quantifying distances. Then, two topographic images are acquired with each tip and the offset between the real distance between the tips and the distance measured with the optical system can be determined (fig. 8b).

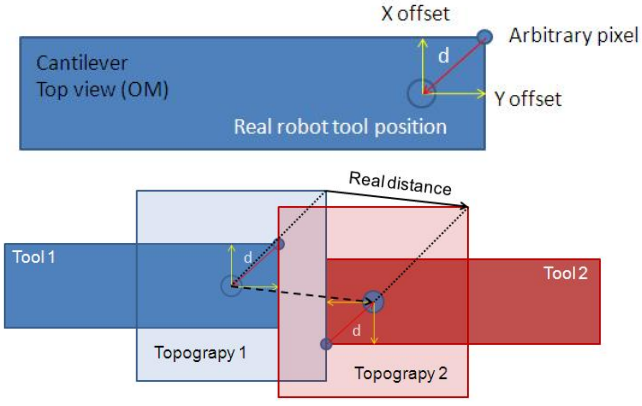

Fig 8. a) Offset between measured and real position of the tool. b) offset calibration by correlating two topographic images

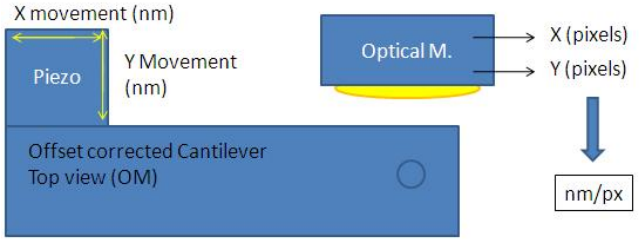

Fig 9. Optical scale factor measurement

Once the correspondence between the two frames is estimated, the true pixel size must be calibrated, due to the tolerances in the devices and tools. The use of a calibration pattern of known size is not suitable in our case because the optical reference plane and the reference planes of the robots change from one experiment to another. For this reason, the pixel size is calibrated at the beginning of every experiment by moving a controlled distance the piezoactuators in a closed loop way (the repeatability of these actuators is better than 25nm in the X and Y direction). The pixel size value can be estimated measuring the displacement with the optical microscope and comparing it with the real movement done by the piezoactuator (figure 9). This last experiment will be presented in the following section in order to proof the resolution of the system in determining the distance between the two robots tools.

III. Experimental Results

The procedure used to estimate the precision of the optical image based AFM tip locating method is to realize several movements with one of the AFM tips, while the other tip is maintained steady. The proposed AFM optical image tip positioning method gives the distance (in pixels) between the two tips in order to be less dependent on the camera vibrations. Nine displacements of the AFM tip were measured: 5000, 3000, 1000, 800, 600, 500, 400, 300 and 200 nm. Twenty measurements were made in each position, in both direction X and Y, giving the mean values shown in the table (1). The graphic results in fig. 9 show the linear relationship between the measured and the effective displacements.

Displ. nm	Mean Displ. X (pixels)	Mean Displ. Y (pixels)
5000	21.33	20.75
3000	12.56	12.39
1000	4.24	4.24
800	3.13	3.27
600	2.86	2.71
500	2.38	1.95
400	1.62	1.67
300	1.24	1.48
200	1.06	1.09

Table 1. AFM tip displacements and the corresponding image measurements (X and Y direction)

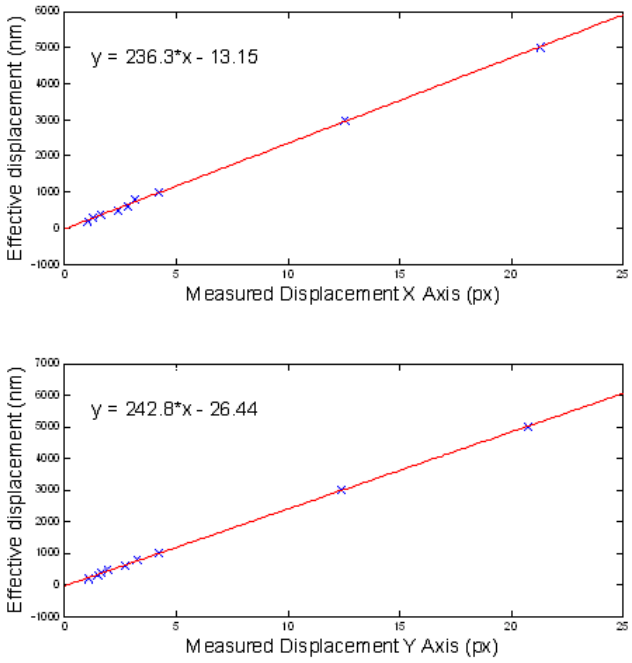

Fig 9. Correspondence between the measured and the effective displacements

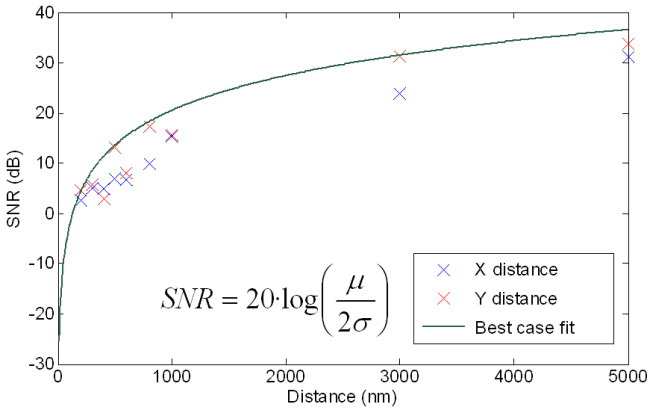

Fig. 10. Signal-to-noise of the detection system in function of the displacement axis, Y axis and best case fit.

The value for displacement per pixel unit is 237.6 nm/px (5000 nm / 21.04 px). The resolution of the detection system is the minimum movement that is effectively detected. Tests show good response to movements of 200nm. But more important than the resolution is the accuracy, defined by the statistical error in a concrete measurement. It is commonly accepted that 2σ (where σ is the standar desviation of the measurement) is a good estimator of the accuracy in a measurement. Test performed in the 5000nm movements have shown a 2σ parameter of 0.53px (128nm). With this best fit estimation, experimental results in X and Y distance measurement are compared in figure 10.

The SNR is low in general due to the physical limits of the system (diffraction limit for the optical microscope and vibration for the CCD sensor) In the measurements can be

observed that the SNR decreases dramaticaly to unaceptable values (less than 10dB) with measurement of distance changes of 300nm. So, movements or distances greather than 300nm can be measured (resolution of the system) with an statistical error (accuracy of the system, 95.4% of the measurements will have an error lower than this limit) is 128nm.

IV. CONCLUSIONS

Micro-to-nano optical resolution is a key objective in a cooperative multirobot nanobiocharacterization station. A multi-robot cooperation station for nano-bio characterization has been presented. The station is composed of two long travel range and high resolution robots equipped with self-sensing nanoprobes that are able to cooperate with each other and with standard AFM systems over a common sample. The robots are guided by the use of an upright high-depth-of-field optical microscope to perform complex experiments [14]. A first nanoprobe is expected to perform a high resolution scanning image and the second one a specific nanomanipulation. The upright optical microscope is used to measure, using computer vision techniques, the correspondence between robot frames.

A first objective has been centered in the optimization of the system for nanocharacterization of bacterial cells when they form biofilms. Optical resolution of 300nm is obtained in the measurement of the relative distance between probes. This result shows that the use of specific computer vision techniques implemented presents an important improvement in the specific conditions of the nanorobotic station (3μm of resolution of the long-working distance optical microscope due to the diffraction limit and 750nm of camera tremor) when geometries of the tools are well defined and calibration procedure is correctly conducted. This is a very important result because it will possible to place the second nanoprobe with respect to the first one with a resolution lower than the radius of the bacterial cell (500nm-1μm) by the use of computer vision techniques.

REFERENCES

[1] A. Alessandrini, P. Facci, “AFM: a versatile tool in biophysics” in Meas. Sci. Tech., vol. 16, 2005, pp. R65-R92.

[2] G. Binning, C.F. Quate, C. Gerber, “Atomic force microscope” in Phys. Rev. Letters, Vol. 56, 1986, pp. 930-933.

[3] D. Anselmetti, “Analysis of subcellular surface structure, function and dynamics” in Anal. Bioanal. Chem., vol. 387, no. 1, 2006, pp. 83-89.

[4] Y. Lyubchenko,A. Gall, S. Shlyaktenko, “Atomic Force Microscopy of DNA and Protein-DNA Complexes Using Fucntionalized Mica Substrates” in Meth. Cell. Sci., vol. 148, 2001, pp. 569-578.

[5] K. A. Whitehead, “Use of atomic force microscope to determine the effect of substratum surface topography on the ease bacterial removal”, in Col. and Surf. B., vol. 51, 2006, pp. 44-53

[6] S. Fatikow, “Development of automated microrobot-based nanohandling stations for nanocharacterization” in Microsys. Technol., vol. 14, 2008, pp. 463-474.

[7] A. Singh, C. Amon, M. Sitti, “Proximal Probes Based Nanorobotic Drawing of Polymer Micro/Nanofibers” in IEEE Trans. Nanotech., vol. 5 no. 5, 2006, 499-510.

[8] R. Donlan, “Role of biofilms in antimicrobial resistance”, in ASAIO Jour., vol. 46, no. 6, 2000, pp. S47-S52.

[9] I. Auerbach *et al.*, “Physical morphology and Surface Proteins of Unsaturated *Pseudomonas Putida* Biofilms”, in Bacteriology, vol. 189, no. 23, 2007, pp. 3809-3815.

[10] M. Sitti, “Atomic Force Microscope Probe Based Controlled Pushing for Nanotribological Characterization” in IEEE Trans. Mech., vol. 9, no. 2, 2004, pp. 343-349.

[11] J. Otero, M. Puig-Vidal, J. Samitier, “Long Travel and High Resolution Nanobiocharacterization Station based on Piezoelectric Actuators”, in Proc. Int. Conf. New Actuators (Actuator08), Bremen, Germany, 2008, pp. 993-996.

[12] J. Otero, M. Puig-Vidal, “Low-noise Instrumentation for the Measurement of Piezoresitive AFM Cantilever Deflection in Robotic Nanobiocharacterization Applications”, in Proc. IEEE Int. Instr. Meas. Technol. Conf. (I2MTC08), Victoria, Canada, 2008, pp. 1392-1396.

[13] M. Guizar-Sicairos, S. T. Thurman, J. R. Fienup, "Efficient subpixel image registration algorithms" in Opt. Lett. vol. 33, 2008, pp. 156-158.

[14] K. Sato, K. Kamiyama, H. Hii, N. Kawakami, S. Tachi, “Measurement of Force Vector Field of Robotic Finger using Vision-based Haptic Sensor”, in Proc. IEEE/RSJ Int. Conf. Intell. Rob. and Systems (IROS08), Nice, France, 2008, pp. 488-493.

[15] Zitová B., Flusser J.: Image registration methods: a survey. Image and Vision Computing, 21 (2003), 11, 977-1000